Original article

Development of starch/chitosan expandable films as a gastroretentive carrier for ginger extract-loaded solid dispersion

Kanidta Kaewkroek [a,b], Arpa Petchsomrit [c], Abdi Wira Septama [d], Ruedeekorn Wiwattanapatapee [a,e,*]

[a] Department of Pharmaceutical Technology, Faculty of Pharmaceutical Sciences, Prince of Songkla University, Hat Yai, Songkhla 90112, Thailand
[b] Faculty of Integrative Medicine, Rajamangala University of Technology Thanyaburi, Thanyaburi, Pathum Thani 12130, Thailand
[c] Department of Pharmaceutical Technology, Faculty of Pharmaceutical Sciences, Burapha University, Bangsaen, Muang, Chonburi 20131, Thailand
[d] Research Center for Chemistry, National Research and Innovation Agency (BRIN), Kawasan Puspiptek Serpong, Tangerang Selatan, Banten 15314, Indonesia
[e] Phytomedicine and Pharmaceutical Biotechnology Excellence Research Center, Faculty of Pharmaceutical Sciences, Prince of Songkla University, Hat Yai, Songkhla 90112, Thailand

ABSTRACT

Gastroretentive expandable films were developed to provide controlled release of ginger extract (GE) for treatment of gastric diseases. The dosage form consisted of ginger extract solid dispersion (GE-SD) loaded in a starch/chitosan composite film, which was subsequently folded and inserted into a hard gelatin capsule. GE-SD was prepared by solvent evaporation using an optimum weight ratio of 1:1 for GE and PVP K30. Expandable films containing GE-SD were prepared by solvent casting combinations of chitosan and either rice-, glutinous rice - or pregelatinized maize starch with glycerin incorporated as a plasticizer. The optimized film formulation prepared from glutinous rice starch, exhibited tensile strength of 5.4 N/cm^2 and high expansion in simulated gastric fluid (SGF), resulting in a 2.8-fold increase in area. The films resulted in sustained release of up to 90% of the content of 6-gingerol during 8 h exposure to SGF. Furthermore, the 6-gingerol released from the film displayed dose-dependent cytotoxic activity against AGS human gastric adenocarcinoma cells and anti-inflammatory activity by inhibiting the production of nitric oxide (NO) in LPS-stimulated RAW264.7 cells.

© 2021 The Author(s). Published by Elsevier B.V. on behalf of King Saud University. This is an open access article under the CC BY-NC-ND license (http://creativecommons.org/licenses/by-nc-nd/4.0/).

1. Introduction

Ginger (*Zingiber officinale* Roscoe, Zingiberaceae) originated in Southeast Asia and has been exploited for over 2000 years because of its medicinal and culinary value. The rhizome of ginger has been used extensively as an ingredient (e.g., spice or flavouring) for a variety of foods and beverages, while the rhizome and its extracts have featured strongly in traditional oriental medicine (Srinivasan 2017). Ginger has been primarily used to treat conditions related to the gastrointestinal tract such as indigestion, nausea, and vomiting (Daud et al., 2011; Sato et al., 2017). Ginger contains a variety of pungent and biologically active compounds featuring gingerols as the major constituents, among which 6-gingerol is the most

abundant (Fitzpatrick and Woldemariam 2017). This phenol phytochemical has been reported to exhibit a number of pharmacological properties including antioxidation, anti-inflammation, gastric protection, antibacterial, and anticancer activity (Ippoushi et al., 2003; Ghasemzadeh et al., 2015; Aslani et al., 2016; Cafino et al., 2016). It is evidenced to be a good scavenger of peroxyl radicals and a potent inhibitor of nitric oxide production and iNOS enzyme induction in lipopolysaccharide (LPS)-stimulated mouse macrophages (Ippoushi et al., 2003). The chemopreventive and chemoprotective effects of 6-gingerol have been shown to be associated with their antioxidative and anti-inflammatory activities (Habib et al., 2008; Hamza et al., 2021). 6-gingerol has also been found to be cytotoxic to various cancer cells lines including human colon cancer (HCT15), fibrosarcoma (L929), and murine macrophages (Raw 264.7) (Kumara et al., 2017). In terms of safety, ginger has been approved by the American Food and Drug administration as a GRAS (Generally Recognized as Safe) ingredient (Ali et al., 2008; Singletary 2010).

Despite their demonstrated pharmacological activity, clinical application of gingerol is restricted due to low aqueous solubility and short half-life, leading to poor oral bioavailability (Jiang et al., 2008). Solid dispersions (SD) are one of the most successful

* Corresponding author.
E-mail address: ruedeekorn.w@psu.ac.th (R. Wiwattanapatapee).
Peer review under responsibility of King Saud University.

Production and hosting by Elsevier

formulation strategies for improving the solubility and bioavailability of poorly water-soluble drugs and are applicable to gingerols. Generally, SDs consist of the drug finely dispersed in a hydrophilic and biocompatible polymer matrix or carrier, such as polyvinyl pyrrolidone (PVP), Eudragit (Kerdsakundee et al., 2015; Wannasarit et al., 2019), polyethylene glycol (PEG), hydroxypropyl methylcellulose (HPMC), and methylcellulose (MC) (Dalvi et al., 2015).

Gastro-retentive drug delivery devices have been designed to prolong drug release in the stomach by different approaches. Expandable systems, for example, are usually folded in a capsule and expand to dimensions greater than the pyloric sphincter upon contact with gastric fluid (Vrettos et al., 2021). Therefore, they remain in the stomach and extend drug release. Numerous devices having various geometrical shapes have been investigated, including rings-, discs, tetrahedrons, and 4 lobed-forms (Mehta et al., 2018). Semi-synthetic and synthetic polymers including HPMC, ethyl cellulose, Eudragit polymers, and polyvinyl alcohol are generally used to produce these gastroretentive devices (Kaewkroek et al., 2019). However, natural polymers offer major advantages due to their non-toxic, biocompatible, and biodegradable properties.

Starch is a naturally occurring polymer, obtained from a variety of plant sources including corn, rice, wheat, and potato. The basic chemical formula is $(C_6H_{10}O_5)_n$ where n is the number of glucose molecules that are connected by α-glycosidic linkages. Starch in its native and modified forms has been used extensively as a pharmaceutical excipient, particularly in tabletting, serving as binder, disintegrant, diluent, glidant, and lubricant (Builders and Arhewoh 2016). Chitosan is a natural carbohydrate polymer obtained by the deacetylation of chitin [poly-β-(1-4)-N-acetyl-D-glucosamine], a major component of crustacean shells (Santos et al., 2020). Chitosan has also been widely investigated as an excipient in various pharmaceutical dosage forms to control disintegration of tablets, for example, or to modify drug release behaviour (Lu et al., 2019; Patil et al., 2021).

Starch is one of the most commonly used materials to prepare films for its low cost, renewable and biodegradability. However, wide application of starch film is limited by its water solubility and brittleness (Wu and Zhang 2001). Therefore, it is often combined with other substances to form polymers with lower solubility and greater mechanical strength. Such polymers include chitosan, cellulose, alginate and xanthan gum (Wu et al., 2019). Mixing chitosan to starch film can improve water resistance, water vapor transmission rate (WVTR), and mechanical strength due to the formation of intermolecular hydrogen bonds between the amino and hydroxyl groups of chitosan and the hydroxyl groups of the starch (Wittaya 2012). Solution casting is one of the commonly used techniques to prepare starch films. The method involves solubility of the biopolymer in a solvent/plasticizer, casting in the mold and drying (Bangar et al., 2021).

In recent years, the starch-chitosan composite films have been widely investigated, primarily for their application as food packaging materials (Lauer and Smith 2020). By contrast, a limited number of applications in drug delivery systems have been reported. Recently, glutinous rice starch-chitosan composite film was found to exhibit an effective coagulation effect, making it an ideal material for blood-stopping wound dressing (Wu et al., 2019). Ball-milling modified glutinous rice starch – chitosan composite films were developed and characterized. The composite films could be useful for buccal delivery of a model hydrophilic drug, lidocaine hydrochloride (Soe et al., 2020). In another study, resveratrol loaded expandable films prepared using pre-gelatinized corn starch and chitosan demonstrate the potential for prolonging drug release in the stomach for treatment of gastric disorders (Boontawee et al., 2021).

The aim of this study was to develop a novel expandable, gastroretentive device, for localized and prolonged release of 6-gingerol in the stomach for the treatment of gastric disorders, based predominantly on natural polymers. Composite expandable films produced from starch and chitosan acted as a stomach-specific carrier for solid dispersions incorporating ginger extract. The physicochemical properties and release behavior of the films were investigated along with the anti-proliferative and anti-inflammatory *in vitro* activities of released 6-gingerol.

2. Materials and methods

2.1. Materials

6-gingerol (98% purity) was obtained from Baoji Herbest Bio-Tech Co., Ltd (Shaanxi, China). GE was purchased from Guangzhou Phytochem Sciences Inc. (Guangzhou, China). Glycerin was from P. C. Drug Center Co., Ltd (Bangkok, Thailand). Pre-gelatinized maize starch (Starch 1,500®; 27.0% amylose content) were provided by Colorcon (Indianapolis, USA). Eudragit® EPO (average MW 150 kDa) was obtained from Evonik Industries AG (Darmstadt, Germany). Rice starch (*Oryza sativa*; 33.8% amylose content) and glutinous rice starch (*Oryza sativa* var. Glutinosa; 0.56% amylose content) were sourced from Cho Heng Rice Vermicelli Factory Co., Ltd. (Nakhon Pathom, Thailand). Chitosan was purchased from Seafresh Industry Ltd. (Bangkok, Thailand). Hard gelatin capsules (size 00) were sourced from Capsugel (Bangkok, Thailand).

AGS cells (human gastric adenocarcinoma cell line) and RAW264.7 cells (murine macrophage cell line) were purchased from the American Type Culture Collection, ATCC (VA, USA). Lipopolysaccharide (LPS, from Escherichia coli) and indomethacin were purchased from Sigma Aldrich (Sigma Aldrich, Missouri, USA). Fetal calf serum (FCS), Roswell Park Memorial Institute 1640 medium (RPMI-1640), Dulbecco's modified Eagle's medium (DMEM), 3-(4,5- dimethyl-2-thiazolyl)-2,5-diphenyl-2H-tetrazo lium bromide (MTT), phosphate buffer saline (PBS), Penicillin-streptomycin were supplied by Gibco (Invitrogen, California, USA). 96-well microplates were obtained from Nunc (Nunc, Birkrød, Denmark). Dimethylsulfoxide (DMSO) was from Amresco (OH, USA). All other chemicals were of analytical or pharmaceutical grades.

2.2. Preparation of ginger extract solid dispersion

The hydrophilic polymers PVP K-30 and Eudragit EPO, respectively, were used to prepare SDs of GE using solvent evaporation (Kerdsakundee et al., 2015; Wannasarit et al., 2019). GE and polymer were weighed in the ratio of 1:1–1:6 and dissolved in methanol to obtain a clear solution. The solvent was removed by rotary evaporation at 40 °C (Heidolph® Instruments GmbH & CO. KG, Schwa Bach, Germany). The dry samples were ground using a mortar and pestle, then sieved to provide a 0.05–0.25 mm particle size fraction. The resulting SDs were kept in air-tight containers at 4 °C and protected from light. Physical mixtures (GE-PM) were prepared by blending the ginger extract and polymer at different weight ratios in a mortar and stored under the same conditions as the SD.

2.3. Solubility of ginger extract solid dispersions

The solubility of each type of GE-SD was determined using the flask shaking method (Kerdsakundee et al., 2015; Bunlung et al., 2021). An excess amount of GE-SD, GE-PM, and ginger extract, respectively, was added to separate vials containing 1 mL of 0.1 N hydrochloric acid (pH 1.2). After capping the vials, the mix-

ture was vortexed (Vortex-Genie 2, 50 Hz model, Scientific Industries Inc., Bohemia, USA) at maximum speed for 10 min. The vials were transferred to a water bath shaker (Julabo® SW22, Seelbach, Germany) and maintained at 37 °C, 100 rpm for 48 h. The mixture was centrifuged at 4000 rpm for 10 min. The supernatant was collected into glass vials, diluted and filtered through a 0.45 μm filter paper and stored at 4 °C prior to analysis.

The concentration of 6-gingerol in the supernatant corresponding to each test sample was measured by HPLC. Aliquots were diluted with methanol and 20 μL of the diluted samples were injected directly on the HPLC column. The quantitative determination of 6-gingerol was performed using an Agilent HPLC photodiode array detector (HP 1100, Agilent, Santa Clara, USA) with a Verti-SepTM UPS C18 5 μm column (4.6–250 mm) (Ligand Scientific, Bangkok, Thailand). The mobile phase (methanol:1% acetic acid (75:25, v/v)) was run isocratically for 16 min at a flow rate of 1 mL/min. The wavelength of detection was 282 nm. The analysis was repeated three times for each formulation and data were reported as mean ± SD. Quantification of 6-gingerol in the supernatant was achieved by comparison with a calibration curve produced using 6-gingerol.

2.4. Characterization of ginger extract solid dispersions

2.4.1. X-ray diffraction studies
X-ray diffraction patterns were obtained at room temperature using an X-ray diffractometer (Philips: X'pert MPD, Amsterdam, Netherlands). Studies were performed under a voltage of 40 kV and a current of 30 mA at a scan speed 1 s/step over a 2θ range of 5–90° using a step size of 0.05°.

2.4.2. Fourier transform infrared (FT-IR) spectroscopy
FT-IR spectra were obtained using a Fourier transform infrared spectrometer (Perkin-Elmer, Waltham, USA) equipped with a deuterated triglycine sulfate detector. Samples were prepared in potassium bromide (KBr) discs. The scanning range was 450–4000 cm^{-1}.

2.5. Preparation of expandable films loaded with ginger extract solid dispersions

The composite, natural polymer expandable films were prepared by solvent casting (Boontawee et al., 2021). Starch (rice starch, glutinous rice starch or pre-gelatinized maize starch) and chitosan were used as film-forming agents while glycerin was included as a film plasticizer. Different concentrations of starch, chitosan, and glycerin (Table 1) were dissolved in 30 mL of acetic acid (1% w/v). The solutions were heated at 90–100 °C for 2 h and stirred overnight at room temperature. GE-SD (2 g) was added, followed by continuous stirring until a homogenous solution was obtained. The resulting solution was poured into a glass petri dish (area 64 cm^2) and allowed to dry at 45 °C for 48 h. The resulting composite films were carefully removed and cut into 40 × 20 mm size rectangles prior to loading into hard gelatin capsules (size 00) by zigzag folding.

2.6. Physicochemical characterization of expandable starch/chitosan films loaded with ginger extract solid dispersions

2.6.1. Film weight and thickness
Each film formulation was prepared in triplicate and rectangular samples (40 × 20 mm) were cut from each preparation. Ten samples were weighed using an analytical balance (Practum224-1s, Sartorius, Goettingen, Germany). Film thickness was measured at five different positions using a digital vernier caliper (V6-154,

Kovet Co, Ltd, Bangkok, Thailand). The mean ± SD values were calculated for all formulations.

2.6.2. 6-gingerol content
Film samples (40 × 20 mm) were immersed in 20 mL of 0.1 N hydrochloric acid (pH 1.2) in a volumetric flask for 1 h to dissolve chitosan, followed by immersion in 80 mL of methanol to extract 6-gingerol from film. After sonication for 30 min, the resulting solutions were filtered through a 0.45 μm filter paper and diluted with methanol. The 6-gingerol content of the solutions was analyzed using HPLC that described earlier in the part of solubility of ginger extract. The test was repeated three times for each formulation and data were reported as mean ± SD.

2.6.3. Measurement of film tensile properties
A texture analyzer (TA.XT plus Texture Analyser, Stable Micro Systems, Surrey, UK) was used to determine film tensile strength. Film strips were held between two clamps positioned 30 mm apart. Card was attached to the surface of the clamps to prevent film breakage by the grooves of the clamp. Samples were extended at a rate of 2.0 mm/s until fracture and the applied force was recorded. Tensile measurements were obtained for six samples of each film formulation. and the tensile strength was calculated according to the following equation.

$$\text{Tensile strength } (N/cm^2) = \text{Force at break } (N)/\text{Initial cross} \\ - \text{sectional area of the sample } (cm^2)$$

2.6.4. Film unfolding behavior and expansion in simulated gastric fluid
Film samples (40 × 20mm) were folded in a zigzag manner and inserted singly into a size 00 hard gelatin capsule. Six loaded capsules were exposed to simulated gastric fluid (SGF) (900 mL, 0.1 N hydrochloric acid, pH 1.2) at 37 ± 0.5 °C using a USP 30 rotating basket dissolution apparatus (Vankel model VK7000, Montréal-Est, Canada) at a rotation speed of 100 rpm. The unfolding behavior of the film was observed at 5, 10, 20, 15, 30, 60, and 480 min. The film dimensions were also measured at 480 min to determine the % film expansion based on area.

2.6.5. Film swelling behavior
The swelling behavior of the films over time was investigated by measuring the weight of samples before (W1) and after (W2) immersion in 200 mL of 0.1 N hydrochloric acid (pH 1.2) at different time points (5, 10, 20, 30, 60, 120, 240, and 480 min). Fluid absorption was expressed as %weight gain according to the following equation and reported as mean ± SD. (n = 3).

$$\text{Fluid absorption} = [(W2 - W1)/W1] \times 100$$

2.6.6. Morphology of ginger extract solid dispersions-loaded films
Scanning electron microscopy (SEM) was used to examine the morphology of GE-loaded film formulations (G5) (JSM-5800LV, Jeol, Tokyo, Japan). Samples were sputter coated with gold prior to examination at 20 keV accelerating voltage.

2.6.7. 6-Gingerol release from starch/chitosan expandable films
The drug release profile of film formulations was determined using USP 30 rotating basket dissolution apparatus at 37 ± 0.5 °C and a rotating speed of 100 rpm in 900 mL of 0.1 N hydrochloric acid. Samples (5 mL) were withdrawn after 10, 20, 30, 60, 120, 240, 360, and 480 min and replace with fresh medium. The samples were filtered and analyzed using the HPLC method. The cumulative percentage release of 6-gingerol from each formulation was calculated. The test was repeated three times for each formulation and data are reported as mean ± SD. The obtained release profiles

Table 1
Composition of GE-SD starch/chitosan expandable films.

Formulation	GE-SD (g)	Glycerin (g)	Pre-gelatinized maize starch (g)	Glutinous rice starch (g)	Rice starch (g)	Chitosan (g)
P1	2	0.7	1	–	–	0.5
P2						0.8
P3			1.25	–	–	0.5
P4						0.8
P5			1.5	–	–	0.5
P6						0.8
G1	2	0.7	–	1	–	0.5
G2						0.8
G3			–	1.25	–	0.5
G4						0.8
G5			–	1.5	–	0.5
G6						0.8
R1	2	0.7	–	–	1	0.5
R2						0.8
R3			–	–	1.25	0.5
R4						0.8
R5			–	–	1.5	0.5
R6						0.8

R: rice starch, G: glutinous rice starch, P: pre-gelatinized maize starch

were analyzed with zero- and first-order kinetics (Wagner 1989) as well as Higuchi (Higuchi 1963) models.

2.7. In vitro cytotoxic activity of 6-gingerol released from films

The cytotoxicity of 6-gingerol released from expandable films was determined using the MTT colorimetric method (Kaewkroek et al., 2019). AGS cells (a human gastric adenocarcinoma cell line) were grown in Dulbecco's Modified Eagle Medium (DMEM, Gibco®, Paisley, UK) supplemented with 10% fetal bovine serum and 1% antibiotics (100 mg/mL streptomycin and 100U/mL penicillin) (Gibco®). The cells were cultured in a humidified condition at 37 °C and 5% CO_2. When the cultures reached 80–90% confluency, the monolayers were washed with PBS (pH = 7.4) and detached with 0.25% trypsin-EDTA solution (Gibco®). Cells were counted using a hemocytometer (Gibco®) and re-plated in 96- well plates (2×10^4 cells/well). After 24 h incubation, the culture medium was removed, and 100 μL of the test sample were added to triplicate wells. Test samples consisted of 'free' 6-gingerol (in DMSO), 6-gingerol released from starch/chitosan films, and GE-SD. After 24 h exposure, 10 μL of MTT solution (5 mg/mL in PBS) were added to each well and incubation was continued for a further 4 h. The MTT reagent was removed and the formazan crystals formed by the viable cells were dissolved by adding DMSO. The spectrophotometric absorbance was measured at 570 nm using a microplate reader (SPECTROstar Nano Microplate Reader, BMG Labtech, Singapore) and cell viability was determined using the following relationship:

$$\text{Cell viability}(\%) = [(\text{OD of sample})/(\text{OD of control})] \times 100$$

The test samples were considered to be cytotoxic when the optical density of the sample-treated group was less than 80% of that in the control (vehicle-treated) group.

2.8. In vitro anti-inflammatory activity of 6-gingerol released from films

The inhibitory effect of released 6-gingerol on nitric oxide (NO) production by murine macrophage-like RAW264.7 cells was evaluated using a modified previously reported method (Kaewkroek et al., 2013). Briefly, RAW264.7 cells were cultured in RPMI medium (Gibco®) supplemented with 0.1% sodium bicarbonate and 2 mM glutamine, penicillin G (100 units/mL), streptomycin (100 μg/mL), and 10% FCS. The cells were harvested with trypsin-EDTA and diluted to a suspension in fresh medium. The cells were seeded in 96-well plates (1×10^5 cells/well) and allowed to adhere for 1 h at 37 °C in a humidified atmosphere containing 5% CO_2. After that, the medium was replaced with fresh medium containing 100 ng/ mL of LPS, together with the test samples at various concentrations, and incubated for 24 h. Test samples comprised of 'free' 6-gingerol (in DMSO), 6-gingerol released from starch/chitosan films, and GE-SD. Indomethacin was used as a positive control. NO production was determined by measuring the accumulation of nitrite in the culture supernatant using Griess reagent and detection of the color at 570 mm. The percentage inhibition of NO production was calculated using the following equation and IC_{50} values were determined ($n = 4$):

$$\text{Inhibition}(\%) = [(A - B)/(A - C)] \times 100$$

A-C: NO_2concentration (μM) [*A*: LPS (+), sample (-); *B*: LPS (+), sample (+); *C*: LPS (-), sample (-)].

2.9. Statistical analysis

All results were expressed as the mean ± SD. Differences between two related parameters were assessed by Student's *t*-test or one-way ANOVA. Differences were considered significant at p < 0.05.

3. Results and discussion

3.1. Preparation of ginger extract solid dispersions and determination of 6-gingerol solubility

Solid dispersions are designed to enhance the solubility of poorly water-soluble compounds by dispersion of fine particles throughout a polymer matrix. In this way, available particle surface area is increased such that wetting and dissolution occur more rapidly (Matteucci et al., 2008). The SD formulation approach also confers advantages of high drug loading and the potential for improving the physicochemical stability of active compounds (Matteucci et al., 2008). SD techniques have previously been applied to a number of hydrophobic herbal compounds including curcumin, Centella extract, and quercetin resulting in a significant improvement in their solubility and therapeutic effect such as

wound healing and anti-inflammatory activities (Kerdsakundee et al., 2015; Wannasarit et al., 2019; Bunlung et al., 2021).

PVP was selected for production of GE-SD due to its high hydrophilicity and good solubility in a wide variety of organic solvents (dos Santos et al., 2021). The dimethylaminoethyl methacrylate-copolymer (Eudragit EPO) dissolves at low pH (pH < 5) (Kerdsakundee et al., 2015) and was investigated as a carrier for GE to improve solubility and release of 6-gingerol in gastric fluid (pH 1.2). GE-SDs were prepared by solvent evaporation using GE:polymer weight ratios of 1:1–1:6. The dried SDs were generally obtained as a fine, yellow powder (Fig. 1). Only SDs prepared from GE and Eudragit using 1:1 or 1:2 w/w ratios displayed unsatisfactory physical appearance and were excluded from further study.

The solubility of 6-gingerol following exposure of GE to SGF was very low and measured as 0.28 ± 0.01 mg/mL. Formulation of GE as physical mixtures with PVP K30 or Eudragit EPO to SGF resulted in improvement of 6-gingerol solubility but values were lower than 1 mg/mL (Figs. 2 and 3). Kumar Singh and Pal Kaur reported a solubility of 3.2 mg/mL for 6-gingerol when GE was exposed to SGF and a reduced solubility of 0.7 mg/mL on exposure to water (Kumar Singh and Pal Kaur 2011). Formulation of GE-SDs resulted in a marked improvement of 6-gingerol solubility in SGF, compared with GE-PM. The solubility decreased with increasing amounts of PVP K30 or Eudragit EPO in the SD and was greater for PVP (22.8 mg/mL at 1:1 GE:polymer ratio) compared with Eudragit (11.9 mg/mL, 1:3 ratio), respectively.

Fig. 1. The appearance of GE-SD powder.

PVP is utilized extensively in solid dispersions to enhance drug solubility because of its capacity to preserve the amorphous state by creating an intermolecular hydrogen bond between drug and polymer (Wang et al., 2017). Saal et al. reported that the solubility of several anionic drugs (indomethacin, warfarin, bezafibrate, and piroxicam) rose as the concentration of Eudragit EPO increased, before plateauing due to steric hindrance of the interactions between Eudragit and the active drug at high polymer loading (Saal et al., 2017). However, the gradual decrease in 6-gingerol solubility in the present study, on raising the proportion of carrier polymer in the SD follows the pattern reported previously for curcumin-Eudragit EPO solid dispersions (Kerdsakundee et al., 2015) and Centella extract-PVP K30/ Eudragit EPO solid dispersions (Wannasarit et al., 2019). This behaviour suggests that dissolution of 6-gingerol may be delayed by the volume of the surrounding polymer which impedes fluid uptake and wetting and prolongs carrier dissolution (Karavas et al., 2006).

3.2. Characterization of ginger extract solid dispersions

The amorphous state of the drug in solid dispersion is critical for increasing their solubility as no energy is required to break the drug crystal lattice (Bhujbal et al., 2021). Therefore, the amorphous form of many poorly water-soluble drugs can achieve substantially higher apparent solubility and markedly faster dissolution. Amorphous solid dispersion also produce supersaturation in the gut resulting in enhancing the drug absorption (Thomas 2020).

3.2.1. X-ray diffraction studies
Powder X-ray diffractograms of GE-SD (1:1 w/w ratio) prepared using PVP K30 displayed a marked absence of peaks corresponding to crystalline components (Fig. 4) whereas the samples of GE-PM and GE gave rise to an abundance of sharp, crystal-associated peaks. The amorphous form of GE-SD correlates with the enhanced solubility of GE-SDs compared with GE-PMs (Fig. 2).

3.2.2. Fourier transform infrared spectroscopy
The FT-IR spectrum of PVP K30 featured important bands at 2956 cm^{-1} (C-H stretch) and at 1660 cm^{-1}, which is attributed to stretching of ⁻CAO group. The band at 1290 cm^{-1} is attributed to the ⁻NOC group. The FT-IR spectrum of GE (Fig. 5) displayed the characteristic features of phenol compounds. A broad band located at 3,421 cm^{-1} was attributed to O–H stretching of hydrogen-bonded hydroxyl groups. Bands at 2928 and 2857 cm^{-1} corresponded to CH$_2$ stretching peaks, a small peak at 1709 cm^{-1} was due to –C = O stretching while bands at 1374 cm^{-1}, 1268 cm^{-1}, 1100 cm^{-1}, and 891 cm^{-1} corresponded to aromatic C–H in-plane deforming and stretching, –C–O–C stretching, and –C–O stretching of –C–O–H bonds, respectively (Aris and Morad 2014). The peak at 1709 cm^{-1} was not present in the spectra of physical mixtures of GE with PVP K30 while the peaks at 3421, 2928, 2857, 1660, 1374, 1268, and 1100 cm^{-1} were shifted to 3426, 2927, 2860, 1661, 1375, 1290, and 1087 cm^{-1}, respectively, indicating the presence of H-bonding between GE and PVP-K30. In the spectra obtained for solid dispersions of GE with PVP K30, the characteristic band of GE shifted from 2928 cm^{-1} to 2926 cm^{-1} and the broad band at 3421 shifted to a higher wave number located at 3425 cm^{-1}. Moreover, the absorption bands of GE at 1709, 1268, and 1100 cm^{-1} were not present. From the above data, interaction was expected between GE and PVP K30 in the solid state, involving the –OH group of GE and the carbonyl group in PVP K30 (Kanaze et al., 2006).
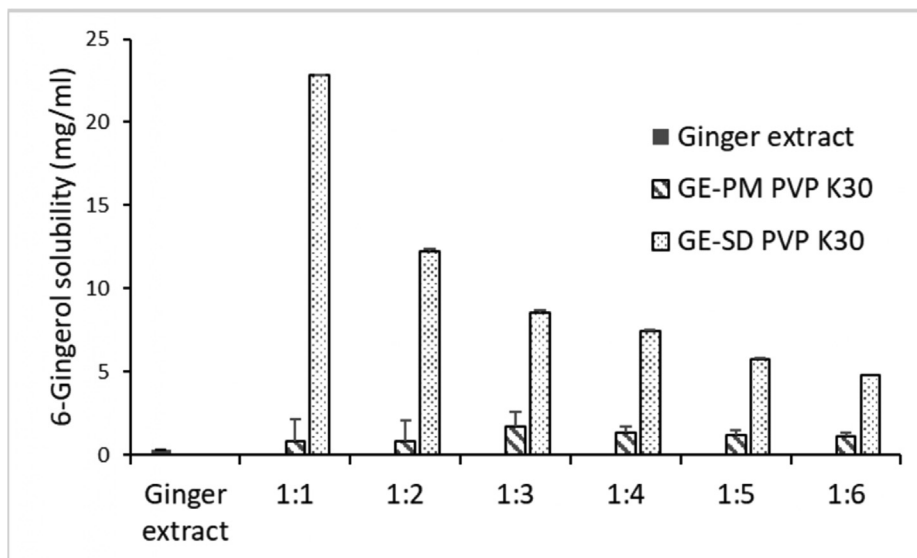
Fig. 2. Solubility of 6-gingerol resulting from formulation of GE:PVP K30 solid dispersions (GE-SD PVP K30) and GE:PVP K30 physical mixtures (GE-PM PVP K30). Solubility testing carried out in 0.1 N hydrochloric acid (pH 1.2), 37 °C.
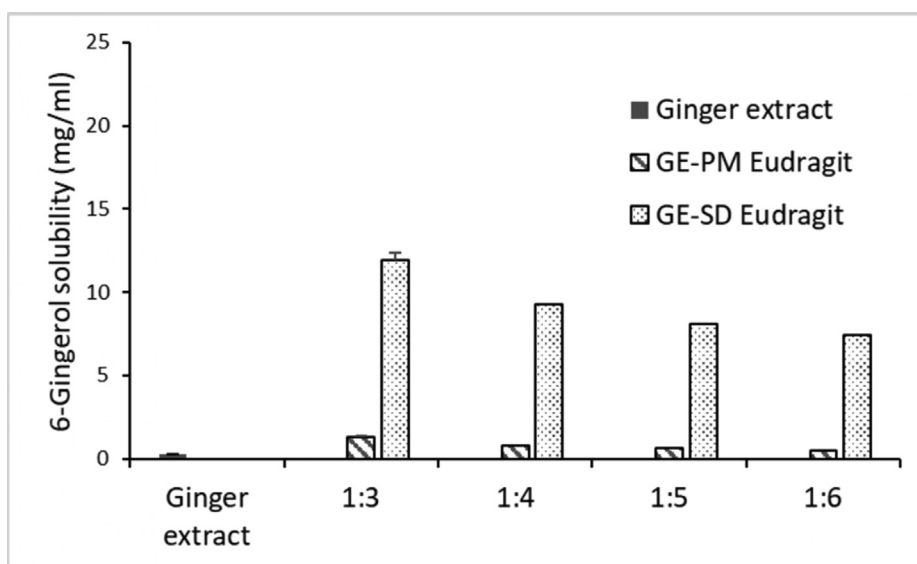
Fig. 3. Solubility of 6-gingerol resulting from formulation of GE:Eudragit EPO solid dispersions (GE-SD Eudragit) and GE:Eudragit physical mixtures (GE-PM Eudragit). Solubility testing carried out in 0.1 N hydrochloric acid (pH 1.2), 37 °C.

3.3. Preparation of starch/chitosan expandable films loaded with ginger extract solid dispersion

GE-SDs prepared from GE and PVP K30 in a 1:1 wt ratio resulted in the highest 6-gingerol solubility in SGF (Fig. 2) and were incorporated in expandable starch/chitosan films. The films were prepared by solvent casting using either rice starch, glutinous rice starch or pre-gelatinized maize starch in combination with chitosan and glycerin included as a film plasticizer. The resulting GE-SD-loaded films were light yellow in color, flexible and tough with smooth surfaces (Fig. 6).

The SEM image of the cross-section of films prepared from glutinous rice starch and chitosan containing GE-SD (Formulation G5) (Fig. 7) displayed a uniform, slightly roughened texture with no sign of large scale voids or cracking or crystal formation. This

indicated that fine particles were homogenously dispersed in the polymeric matrix.

3.4. Physicochemical characteristics of starch/chitosan expandable films containing ginger extract solid dispersion.

3.4.1. Film weight and thickness

The weight of films containing GE-SD ranged from 525.5 ± 0.01 to 649.3 ± 0.02 mg (Table 2) depending on the weight of starch and chitosan utilized, while the mean thickness of films was in the range 0.51 ± 0.01 to 0.75 ± 0.01 mm. The low standard deviation values indicated the good reproducibility of film production and thus high expectation of dosage accuracy (Reyad-ul-ferdous et al., 2015; Domene-López et al., 2019).
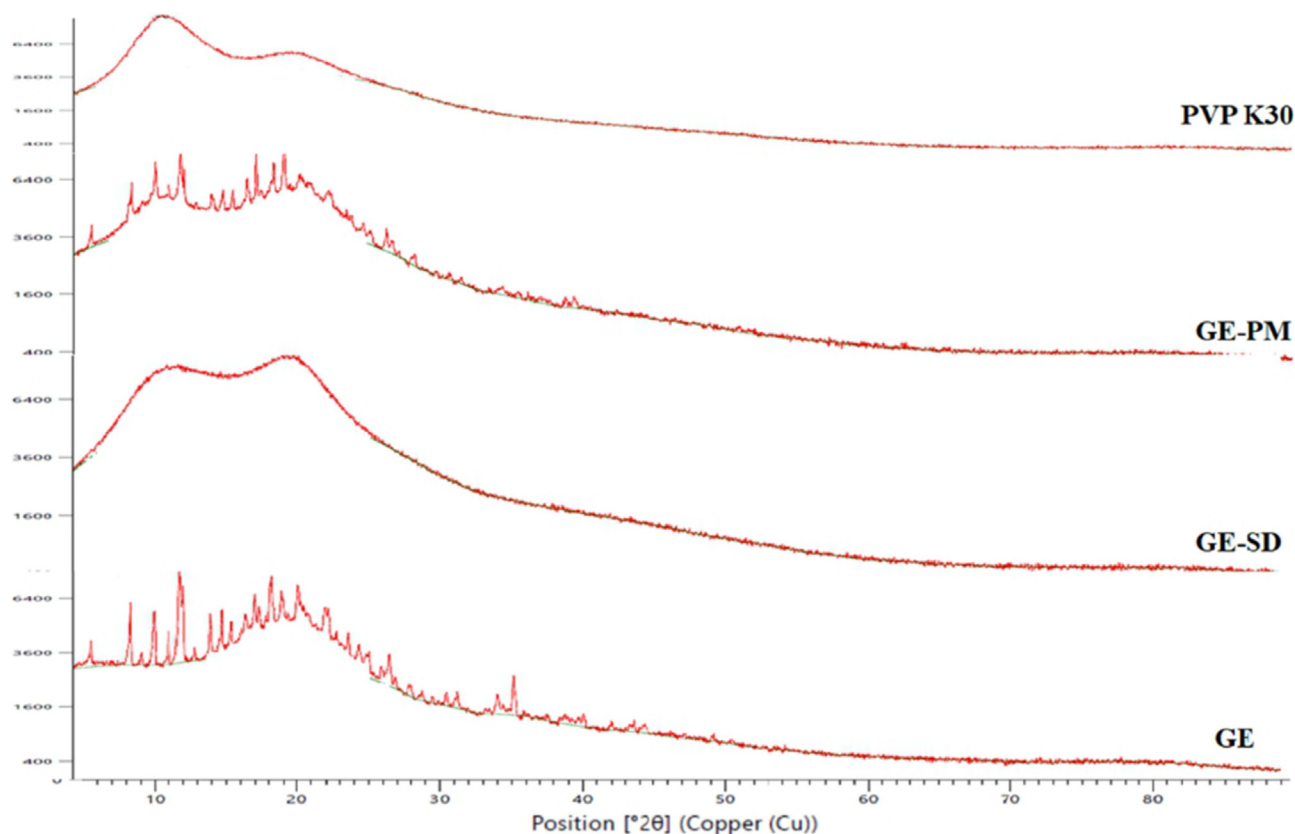
Fig. 4. Powder X-ray diffractograms of PVP K30, 1:1 ginger extract physical mixture (GE-PM), 1:1 ginger extract solid dispersion (GE-SD), and ginger extract (GE), respectively.

3.4.2. Film tensile properties

Expandable dosage forms are designed to have a longer gastric retention time through an increase in their substantial dimension along with high rigidity of the systems to withstand peristalsis and mechanical contractility of the stomach (Prajapati et al., 2013). Tensile strength is a characteristic that indicates the strength and elasticity of the films. The films with high tensile strengths should have better resistance to breaking or disintegration for a substantial period during the drug release in the stomach than those with low tensile strength. The tensile strength of films prepared from pregelatinized maize starch and chitosan occupied a fairly narrow range of 3.6–6.3 N/cm^2 (Table 2). The rise in value reflected the increase of starch and chitosan in the formulation, which resulted in thicker and thus stronger films. Samples prepared from glutinous rice starch and chitosan resulted in the strongest films with maximum strength of 13.8 N/cm^2. These particular formulations also demonstrated a significant influence of the starch and chitosan content on film strength. Increasing the chitosan content from 0.5 to 0.8 g, for example, resulted in 10 times increase in tensile strength (compare formulations G1 and G2). The effect of chitosan content was less pronounced in films produced using rice starch although a similar maximum tensile strength of 11.8 N/cm^2 was obtained.

Our findings support those of Xu et al. who reported an increase in tensile strength of rice starch/chitosan composite films with the addition of chitosan, which was explained by the formation of intermolecular hydrogen bonds between starch and chitosan (Xu et al., 2005). However, too high chitosan concentration resulted in inferior mechanical characteristics. This was due to the occurrence of intramolecular hydrogen bonding rather than intermolecular hydrogen bonds between polymers.

3.4.3. Unfolding behavior of starch/chitosan films in SGF and size expansion

Film samples were folded in a zigzag manner and inserted in hard gelatin capsules. Dissolution of the capsule in SGF subsequently allowed release and gradual unfolding of the polymer film over 5–10 min. Complete unfolding occurred in 15 min. All film formulations showed similar unfolding characteristics. An increase in film thickness was observed in 30 min due to swelling of the polymer and the film maintained good integrity for up to 8 h exposure to SGF (Fig. 8).

Film samples generally exhibited expansion of 2–3 fold on exposure to SGF (Table 2). The maximum expansion (3.7-fold) was displayed by low weight films prepared using glutinous rice starch and chitosan (Formulation G1). However, these films were also characterized by the lowest tensile strength (0.8 N/cm^2), indicating poor physical integration of the starch and chitosan polymers.

The swelling behavior of expandable film (represented as % weight gain in SGF) is depicted in Fig. 9. Films were prepared using glutinous rice starch and chitosan and contained GE-SD (Formulation G5, Table 1). Rapid and considerable swelling occurred in one hour and equilibrium appeared to be reached after 2 h of exposure to SGF. The film thickness increased in 30 min due to the swelling action but remained intact for 8 h in the gastric medium.

Swelling of the films is initially considered to involve "primary bound water" due to hydrogen bonding between water molecules and hydrophilic (–OH) groups in starch and chitosan and amide groups (–NH) in chitosan. Following hydration of the polymer network hydrophobic groups interact with water, resulting in "secondary bound water". 'The quantity of 'total bound water' increases until equilibrium swelling is achieved and the free space
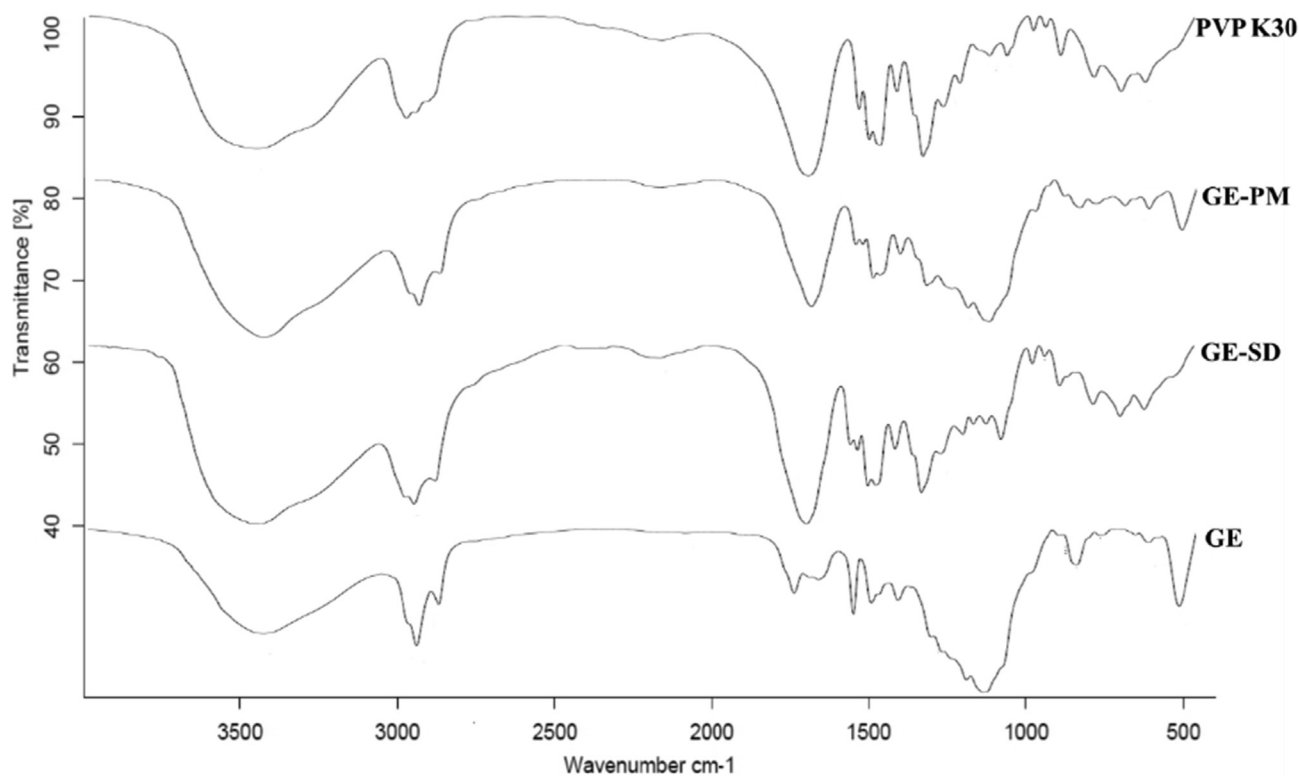
Fig. 5. FT-IR spectrum of PVP K30, ginger extract physical mixture (GE-PM), ginger extract solid dispersion (GE-SD), and ginger extract (GE).
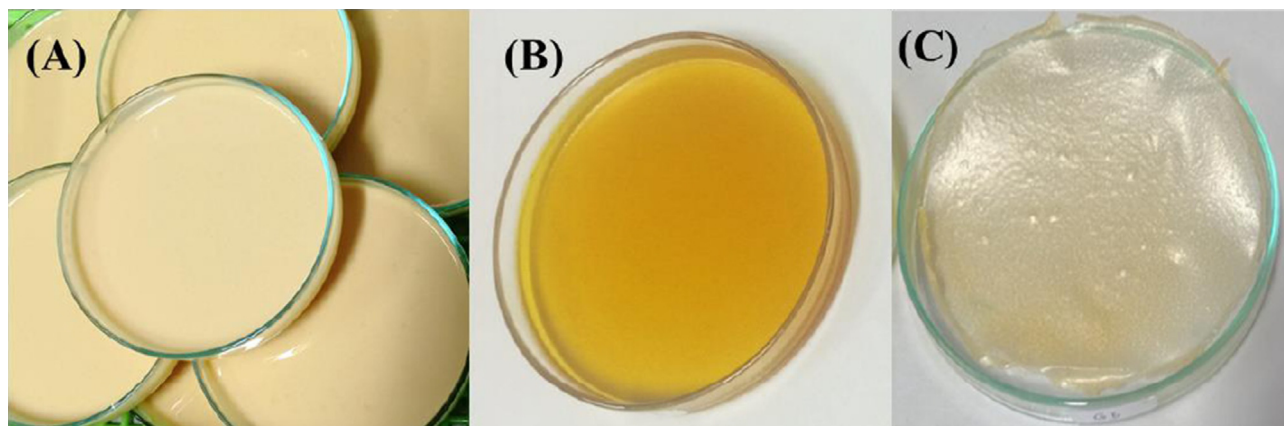

Fig. 6. The appearance of expandable films prepared from glutinous rice starch and chitosan containing GE-SD (Formulation G5). (A) before drying (B) after drying (C) Dried film prepared without inclusion of GE-SD.

including that between network chains and pores or voids is occupied by ''free' or ''bulk' water (Llanes et al., 2020).

Film swelling capacity is influenced by a variety of factors, including the type of monomers, and crosslinking density (Pérez-Álvarez et al., 2018). Chitosan is classed as a homopolysaccharide due to its single monosaccharide constituent whereas starch is a heteropolysaccharide made up of amylose (semicrystalline) and amylopectin (crystalline) components in different proportions depending on the plant species (Rajeswari et al., 2020). Cano and co-workers reported that the amylose to amylopectin ratio is the most important factor in determining film swelling characteristics and *in vitro* drug release rate (Cano et al., 2014). The amylose content of each type of starch employed in this study

is 33.8% (rice), 27.0% (pregelatinized maize), and 0.6% (glutinous rice), respectively. Previous reports suggested that swelling power of starch is contributed by the content of amylopectin (Tester and Morrison 1990, Yuan et al., 2007). In this study, films prepared using glutinous rice which contain the highest amylopectin content exhibit high water absorption (Fig. 9) and high expansion characteristics (Table 2) resulting in higher release rate of drug than other types of films.

3.4.4. 6-gingerol content of starch/chitosan films containing GE solid dispersion

The content of 6-gingerol in the starch/chitosan films containing GE-SD was analyzed using HPLC. The average content varied
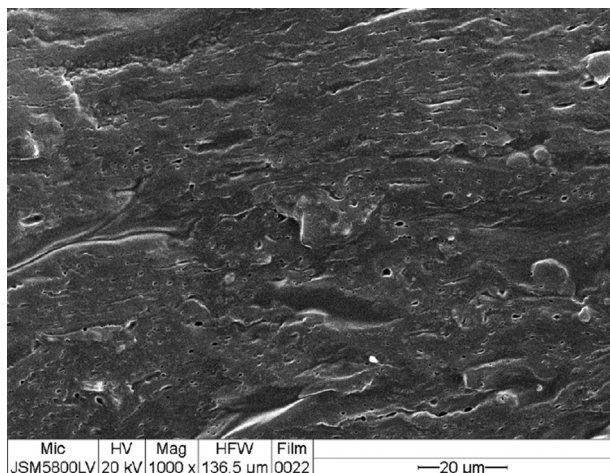
Fig. 7. SEM image of the cross-section of films prepared from glutinous rice starch and chitosan containing GE-SD (Formulation G5).

from 10.4 to 12.6 mg (Table 2) with no significant differences measured between film types i.e., those prepared using pregelatinized maize starch, rice starch or glutinous rice starch. The calculated % drug content was found to be 95.5–98.9%. which were in the similar range with other previous reports i.e., the losartan content in expandable films was 97.4 to 98.8%, whereas resveratrol content was 91.4–103.0% (Kaewkroek et al., 2019; Sah et al., 2020). There is not much deviation in the drug content as the procedure of solvent casting method does not involve any drug loss like other methods of film forming. Moreover, content uniformity testing revealed that 6-gingerol was dispersed evenly throughout the film because the % relative standard deviation was not over 6% (Sevinç Özakar and Özakar 2021).

3.4.5. Release of 6-gingerol from starch/chitosan expandable films

All film formations displayed similar release profiles, consisting of gradual release of 6-gingerol over 8 h exposure to SGF, resulting in high delivery efficiencies of 60–100%. (Fig. 10A-C). Release of 6-gingerol from films prepared from pregelatinized maize starch and chitosan was limited to 60–80% in 8 h, suggesting a lower swelling
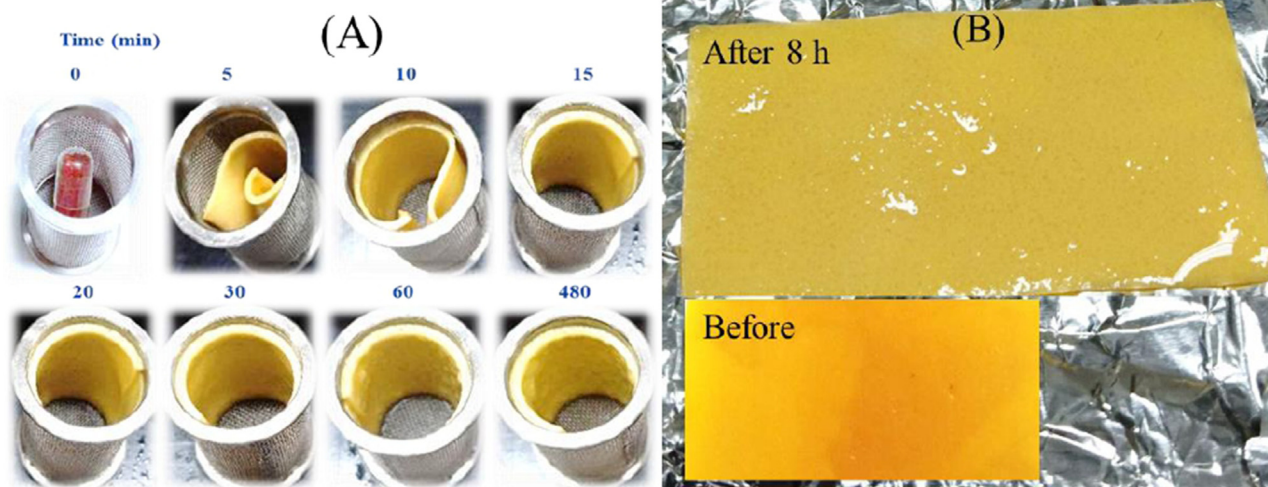
Table 2
Physical properties and 6-gingerol content of expandable starch/chitosan films containing ginger extract solid dispersion.

Formulation	Weight (mg)	Thickness (mm)	6-gingerol content (mg)	Film expansion (fold)	Tensile strength (N/cm^2)
P1	525.5 ± 0.01	0.55 ± 0.01	10.4 ± 0.1	2.28 ± 0.04	3.75 ± 1.00
P2	581.7 ± 0.03	0.62 ± 0.01	10.8 ± 0.4	2.57 ± 0.06	4.46 ± 0.61
P3	559.8 ± 0.01	0.56 ± 0.02	11.2 ± 0.3	2.41 ± 0.04	3.96 ± 0.61
P4	649.3 ± 0.02	0.68 ± 0.02	11.7 ± 0.2	2.57 ± 0.10	4.42 ± 0.77
P5	612.2 ± 0.03	0.65 ± 0.02	12.1 ± 0.2	2.35 ± 0.04	3.59 ± 1.31
P6	664.8 ± 0.02	0.75 ± 0.01	12.6 ± 0.4	2.35 ± 0.06	6.26 ± 1.50
G1	507.9 ± 0.04	0.52 ± 0.02	10.5 ± 0.9	3.69 ± 0.07	0.82 ± 0.35
G2	578.2 ± 0.03	0.62 ± 0.03	10.9 ± 0.4	2.23 ± 0.02	7.98 ± 0.49
G3	531.5 ± 0.01	0.52 ± 0.02	10.6 ± 0.5	3.44 ± 0.03	2.10 ± 2.64
G4	620.2 ± 0.02	0.67 ± 0.02	11.2 ± 0.1	2.19 ± 0.04	9.36 ± 1.02
G5	563.4 ± 0.02	0.57 ± 0.01	11.4 ± 0.6	2.81 ± 0.02	5.43 ± 1.51
G6	649.8 ± 0.04	0.74 ± 0.03	11.8 ± 0.6	2.49 ± 0.02	13.79 ± 1.67
R1	523.5 ± 0.02	0.51 ± 0.01	11.1 ± 0.1	2.83 ± 0.05	1.27 ± 0.48
R2	587.5 ± 0.03	0.56 ± 0.02	11.9 ± 0.3	2.93 ± 0.15	4.72 ± 1.37
R3	556.9 ± 0.04	0.54 ± 0.01	12.2 ± 0.2	2.89 ± 0.07	3.64 ± 0.52
R4	603.6 ± 0.01	0.60 ± 0.02	11.7 ± 0.3	2.39 ± 0.12	6.06 ± 0.60
R5	593.3 ± 0.03	0.57 ± 0.01	12.6 ± 0.3	2.33 ± 0.01	3.32 ± 0.74
R6	648.3 ± 0.02	0.68 ± 0.02	12.1 ± 0.6	2.33 ± 0.01	11.82 ± 2.44

P = pregelatinized maize starch, G = glutinous rice starch, R = rice starch
All values are means ± SD, n = 10 for weight and thickness, n = 3 for 6-gingerol content and tensile film strength.

Fig. 8. Unfolding behavior of starch/chitosan films containing GE-SD at different time points in 0.1 N hydrochloric acid (pH 1.2) (A) and size expansion (B).
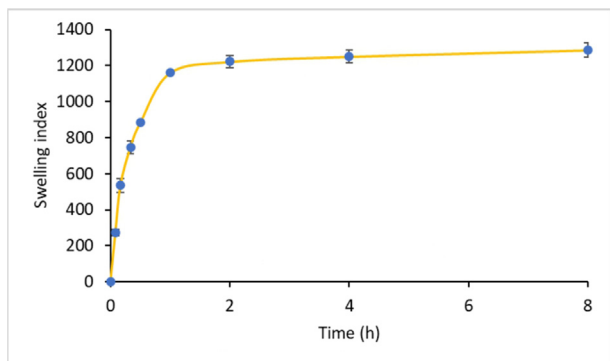
Fig. 9. Swelling behavior of expandable film prepared using glutinous rice starch and chitosan containing GE-SD (Formulation G5).
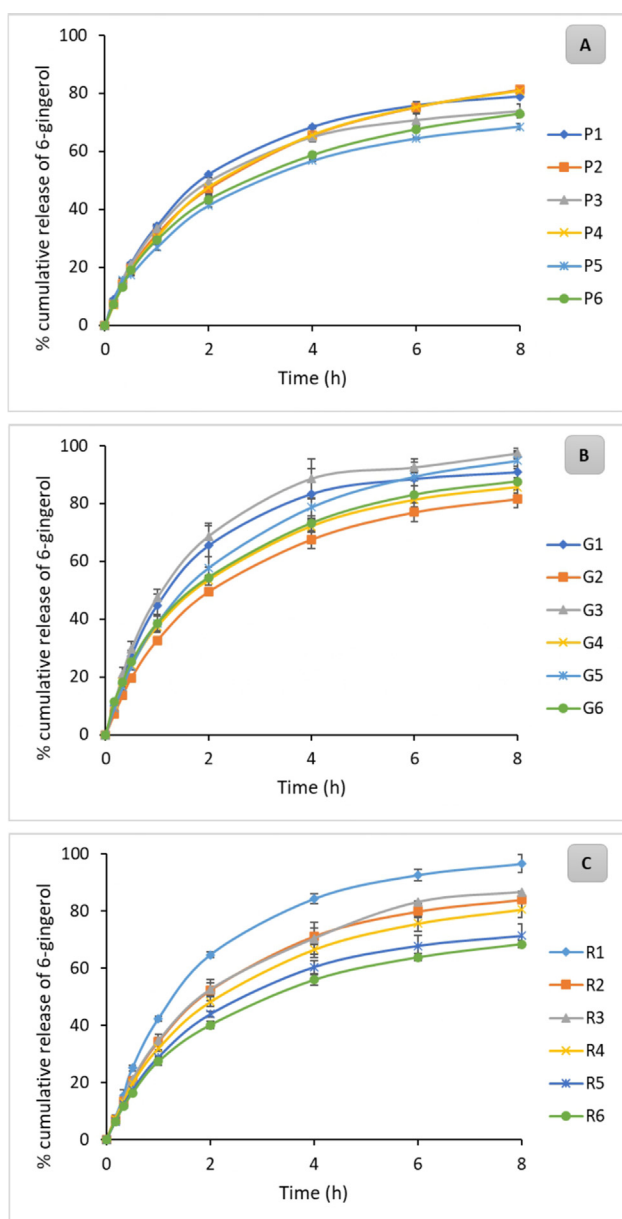

Fig. 10. Release profiles of 6-gingerol from starch/chitosan films prepared using pregelatinized maize- (A), glutinous rice- (B) and rice starch (C) and containing GE solid dispersion. Release medium: 0.1 N hydrochloric acid (pH 1.2), 37 °C.

Table 3

Correlation of 6-gingerol release data obtained using glutinous rice starch/chitosan films with different kinetic models. (Formulation: G5).

Kinetic model	Zero-order $Q_t = K_0t$	First-order $logQ_t = logQ_0 - K_1t/2.303$	Higuchi $Q = K_Ht^{1/2}$
R^2	0.8767	0.4921	0.9808

behavior compared with films containing rice starch or glutinous rice starch, which showed a capacity for 100% gingerol delivery.

The release profiles obtained for films prepared using glutinous rice starch and chitosan (Fig. 10B) revealed some effect of chitosan content on 6-gingerol release behaviour. Film formulations containing lower weights of chitosan (0.5 g) (Formulations G1, G3, and G5) exhibited higher rate of drug release than formulations with higher chitosan content (0.8 g) (Formulations G2, G4, and G6) and almost complete release was measured in 8 h. The higher content of chitosan could render the films stiffer (presented as tensile strength values in Table 2) due to the network formation between starch with chitosan, which prevented water molecules into the films (Wittaya 2012; Boontawee et al., 2021) leading to a lower drug release.

The effect of chitosan content seemed to be less pronounced for the films prepared using rice starch. Rice starch with high amylose content has lower fluid absorption property compared to glutinous rice. The release profiles (Fig. 10C) showed a more relationship with film weight. Almost complete release of 6-gingerol was measured in 8 h for Formulation R1 (524 mg) but was reduced to around 60% for Formulation R6 (648 mg), indicating that 6-gingerol migration through the film was controlled by the density of the swollen network between starch and chitosan.

3.4.6. Mechanism of 6-gingerol release from expandable starch/chitosan films

The 6-gingerol release data presented in Fig. 10 were fitted to the zero-order, first-order, and Higuchi kinetic release models (Sivaneswari et al., 2017) to investigate the underlying release mechanism. Application of the Higuchi model resulted in the strongest correlation ($R^2 = 0.9808$) with the collected data (Table 3). Drug release from matrix-type delivery systems is often controlled by Fickian diffusion and described by the Higuchi, square root of time, kinetic equation (Mircioiu et al., 2019). The modelling study suggested that release of 6-gingerol from the polymeric films was regulated by diffusion through a swollen polymer network characterized by 'bound' and 'free' water content as described earlier (Llanes et al., 2020).

Expandable films prepared from glutinous rice starch and chitosan film containing GE-SD (Formulation G5) exhibited high expansion in SGF (2.8-fold), tensile strength 5.4 N/cm² and almost complete release of 6-gingerol in 8 h exposure to SGF. Samples were subjected to *in vitro* biological assay to assess their potential cytotoxic and anti-inflammatory activity.

3.5. Cytotoxicity of 6-gingerol released from starch/chitosan expandable films

The cytotoxic activity of 6-gingerol released from expandable glutinous rice starch/chitosan films (Formulation G5) was assessed using AGS cells at concentrations of 10–200 µg/mL. The cytotoxicity profile was observed to be dose-dependent with an IC$_{50}$ value of 136.1 µg/mL, comparable with that of free 6-gingerol (in DMSO) (Table 4). The reason for the slightly lower IC$_{50}$ value (122.5 µg/mL) obtained for 6-gingerol released from GE-SD is unclear but may be due to some interference from the film-forming polymer. Overall, the results demonstrate that 6-gingerol released from expandable starch/chitosan films exhibit cytotoxic activity and

Table 4
Anti-inflammatory activity and cytotoxicity of 6-gingerol released from starch/chitosan expandable films.

Test sample	Cytotoxicity(AGS cell assay)IC$_{50}$ (μg/ml)	Anti-inflammatory activity (NO assay)IC$_{50}$ (μg/ml)
G5	136.1 ± 0.9	20.5 ± 0.8
G5-blank	>400	>100
GE-SD	122.5 ± 0.5	18.8 ± 1.3
6-gingerol	132.1 ± 0.8	18.1 ± 0.6
Indomethacin	–	18.8 ± 0.4

[a]Each value represents mean ± SD of four determinations.
G5: 6- gingerol released from starch/chitosan film containing GE-SD (Formulation G5) GE-SD: 6-gingerol released from GE-SD

suggest a potential clinical application of the gastro-retentive delivery system for treatment of stomach cancer.

Our findings support those of Luo et al. who reported that 6-gingerol could reduce the viability of human gastric cancer cells (HGC-27) in a dose-dependent manner (Luo et al., 2018). Mahady et al. reported that ginger root extracts containing gingerols inhibited growth of *H. pylori* CagA + strains *in vitro* and this activity may contribute to its chemopreventive effects against colon cancer (Mahady et al., 2003). Kumara et al. showed that 6-gingerol was cytotoxic to three different cancer cells lines with IC$_{50}$ values of 100 μM for HCT15, 102 μM for L929, and 102 μM for Raw 264.7 cells (Kumara et al., 2017).

3.6. Anti-inflammatory activity of 6-gingerol released from starch/chitosan expandable films

Ginger has been shown previously to be a potent inhibitor of nitric oxide production and iNOS enzyme induction in lipopolysaccharide (LPS)-stimulated J774.1 mouse macrophages cells (Ippoushi et al., 2003). Habib et al. reported that ginger extract significantly reduced expression of NF-κB and TNF-α in rats with liver cancer. Thus, ginger may act as an anti-cancer and anti-inflammatory agent by inactivating NF-κB through the suppression of the pro-inflammatory TNF-α (Habib et al., 2008).

In the present study, the anti-inflammatory activity of 6-gingerol released from glutinous rice starch/chitosan films (Formulation G5) in SGF was assessed by measuring the inhibitory activity against NO production by murine macrophage-like RAW264.7 cells. 6-gingerol released from starch/chitosan films inhibited NO production with an IC$_{50}$ value of 20.5 μg/mL, whereas blank films showed very weak activity (IC$_{50}$ > 100 μg/mL) (Table 4). The NO inhibitory activity of 'free' 6-gingerol (in DMSO) or 6-gingerol released from starch/chitosan films or GE-SD, respectively, was comparable with that of indomethacin (in DMSO), a clinically used NSAIDs. Moreover, RAW264.7 cell viability (as determined using the MTT assay) was not affected at the highest test concentration (100 μg/mL).

4. Conclusions

Expandable films made from starch and chitosan containing ginger extract solid dispersion were successfully prepared by solvent casting for application as gastroretentive delivery systems. The film was designed for oral administration in hard gelatin capsules and unfolded completely within 15 min of exposure to SGF. Gradual release of up to 90% of the 6-gingerol content occurred in SGF over 8 h. The released compound exhibited dose-dependent cytotoxic activity against AGS human gastric cancer cells and anti-inflammatory activity by inhibiting NO production in RAW264.7 cells. The novel gastro-retentive delivery devices based on natural polymers are promising carriers for local delivery of poorly water-soluble compounds in the stomach.

References

Ali, B.H., Blunden, G., Tanira, M.O., Nemmar, A., 2008. Some phytochemical, pharmacological and toxicological properties of ginger (Zingiber officinale Roscoe): a review of recent research. Food Chem. Toxicol. 46 (2), 409–420. https://doi.org/10.1016/j.fct.2007.09.085.

Aris, N.I.A., Morad, N.A.M., 2014. Effect of extraction time on degradation of bioactive compounds (Zingiber Officinale Roscoe). Jurnal Teknologi. 67. https://doi.org/10.11113/jt.v67.2800.

Aslani, A., Ghannadi,A., Rostami, F., 2016. Design, formulation, and evaluation of ginger medicated chewing gum. Adv. Biomed. Res. 5, 130–130. 10.4103/2277-9175.187011.

Bangar, S.P., Purewal, S.S., Trif, M., Maqsood, S., Kumar, M., Manjunatha, V., Rusu, A. V., 2021. Functionality and applicability of starch-based films: An eco-friendly approach. Foods 10 (9), 2181. https://doi.org/10.3390/foods10092181.

Bhujbal, S.V., Mitra, B., Jain, U., Gong, Y., Agrawal, A., Karki, S., Taylor, L.S., Kumar, S., (Tony) Zhou, Q.i., 2021. Pharmaceutical amorphous solid dispersion: A review of manufacturing strategies. Acta Pharm. Sin. B. 11 (8), 2505–2536.

Boontawee, R., Issarachot, O., Keawkroek, K., Wiwattanapatapee, R., 2021. Foldable/expandable gastro-retentive films based on starch and chitosan as a carrier for prolonged release of resveratrol. Curr. Pharm. Biotechnol. 22. https://doi.org/10.2174/1389201022666210615115553.

Builders, P.F., Arhewoh, M.I., 2016. Pharmaceutical applications of native starch in conventional drug delivery. Starch - Stärke. 68 (9-10), 864–873. https://doi.org/10.1002/star.201500337.

Bunlung, S., Nualnoi, T., Issarachot, O., Wiwattanapatapee, R., 2021. Development of raft-forming liquid and chewable tablet formulations incorporating quercetin solid dispersions for treatment of gastric ulcers. Saudi Pharm. J. 29 (10), 1143–1154. https://doi.org/10.1016/j.jsps.2021.08.005.

Cafino, E.J.V., Lirazan, M.B., Marfori, E.C., 2016. A simple HPLC method for the analysis of [6]-gingerol produced by multiple shoot culture of ginger (Zingiber officinale). Int. J. Pharmacog. Phytochem. Res. 8, 38–42.

Cano, A., Jiménez, A., Cháfer, M., Gónzalez, C., Chiralt, A., 2014. Effect of amylose: amylopectin ratio and rice bran addition on starch films properties. Carbohydr. Polym. 111, 543–555. https://doi.org/10.1016/j.carbpol.2014.04.075.

Dalvi, P.B., Gerange, A.B., Ingale, P.R., 2015. Solid dispersion: Strategy to enhance solubility. J. Drug Deliv. Therapeut. 5. https://doi.org/10.22270/jddt.v5i2.1060.

Daud, AnwarS, Bonde, MinalN, Sapkal, NidhiP, 2011. Development of Zingiber officinale in oral dissolving films: Effect of polymers on in vitro, in vivo parameters and clinical efficacy. Asian J. Pharm. 5 (3), 183. https://doi.org/10.4103/0973-8398.91995.

Domene-López, D., García-Quesada, J.C., Martin-Gullon, I., Montalbán, M.G., 2019. Influence of starch composition and molecular weight on physicochemical properties of biodegradable films. Polymers. 11 (7), 1084. https://doi.org/10.3390/polym11071084.

dos Santos, K.M., de Melo Barbosa, R., Meirelles, L., Vargas, F.G.A., da Silva Lins, A.C., Camara, C.A., Aragão, C.F.S., de Lima Moura, T.F., Raffin, F.N., 2021. Solid dispersion of β-lapachone in PVP K30 and PEG 6000 by spray drying technique. J. Therm. Anal. Calorim. 146 (6), 2523–2532. https://doi.org/10.1007/s10973-020-10473-9.

Fitzpatrick, L.R., Woldemariam, T., 2017. Small-molecule drugs for the treatment of inflammatory bowel disease. In: Comprehensive Medicinal Chemistry III. Elsevier, pp. 495–510. https://doi.org/10.1016/B978-0-12-409547-2.12404-7.

Ghasemzadeh, A., Jaafar, H.Z.E, Rahmat, A., (2015). Optimization protocol for the extraction of 6-gingerol and 6-shogaol from Zingiber officinale var. rubrum Theilade and improving antioxidant and anticancer activity using response surface methodology. BMC Compl. Alternat. Med. 15, 258–258. 10.1186/s12906-015-0718-0.

Habib, S.H.M., Makpol, S., Hamid, N.A.A., Das, S., Ngah, W.Z.W., Yusof, Y.A.M., 2008. Ginger extract (Zingiber officinale) has anti-cancer and anti-inflammatory effects on ethionine-induced hepatoma rats. Clinics. 63 (6). https://doi.org/10.1590/S1807-59322008000600017.

Hamza, A.A., Heeba, G.H., Hamza, S., Abdalla, A., Amin, A., 2021. Standardized extract of ginger ameliorates liver cancer by reducing proliferation and inducing

apoptosis through inhibition oxidative stress/ inflammation pathway. Biomed. Pharmacother. 134, 111102. https://doi.org/10.1016/j.biopha.2020.111102.

Higuchi, T., 1963. Mechanism of sustained-action medication. Theoretical analysis of rate of release of solid drugs dispersed in solid matrices. J. Pharm. Sci. 52 (12), 1145–1149. https://doi.org/10.1002/jps.2600521210.

Ippoushi, K., Azuma, K., Ito, H., Horie, H., Higashio, H., 2003. [6]-Gingerol inhibits nitric oxide synthesis in activated J774.1 mouse macrophages and prevents peroxynitrite-induced oxidation and nitration reactions. Life Sci. 73 (26), 3427–3437. https://doi.org/10.1016/j.lfs.2003.06.022.

Jiang, S.-Z., Wang, N.-S., Mi, S.-Q., 2008. Plasma pharmacokinetics and tissue distribution of [6]-gingerol in rats. Biopharm. Drug Dispos. 29 (9), 529–537. https://doi.org/10.1002/bdd.638.

Kaewkroek, K., Tewtrakul, S., Wiwattanapatapee, R., 2019. Development of expandable, gastro-retentive films for delivery of resveratrol and evaluation of cytotoxic and anti-inflammatory activity. Lat. Am. J. Pharm. 38, 691–700.

Kaewkroek, K., Wattanapiromsakul, C., Kongsaeree, P., et al., 2013. Nitric oxide and tumor necrosis factor-alpha inhibitory substances from the rhizomes of <i>Kaempferia Marginata</i>. Nat. Prod. Commun. 8, 1934578X1300800–1934578X1300800. https://doi.org/10.1177/1934578X1300800904.

Kanaze, F.I., Kokkalou, E., Niopas, I., Georgarakis, M., Stergiou, A., Bikiaris, D., 2006. Dissolution enhancement of flavonoids by solid dispersion in PVP and PEG matrixes: A comparative study. J. Appl. Polym. Sci. 102 (1), 460–471. https://doi.org/10.1002/app.24200.

Karavas, E., Ktistis, G., Xenakis, A., Georgarakis, E., 2006. Effect of hydrogen bonding interactions on the release mechanism of felodipine from nanodispersions with polyvinylpyrrolidone. Eur. J. Pharm. Biopharm. 63 (2), 103–114. https://doi.org/10.1016/j.ejpb.2006.01.016.

Kerdsakundee, N., Mahattanadul, S., Wiwattanapatapee, R., 2015. Development and evaluation of gastroretentive raft forming systems incorporating curcumin-Eudragit® EPO solid dispersions for gastric ulcer treatment. Eur. J. Pharm. Biopharm. 94, 513–520. https://doi.org/10.1016/j.ejpb.2015.06.024.

Kumar Singh, P., Pal Kaur, I., 2011. Development and evaluation of a gastro-retentive delivery system for improved antiulcer activity of ginger extract (<i>Zingiber officinale</i>). J. Drug Target. 19. https://doi.org/10.3109/1061186X.2011.561855.

Kumara, M., Shylajab, M., Nazeemc, P., et al., 2017. 6-Gingerol is the most Potent Anticancerous Compound in Ginger (Zingiber officinale Rosc.). J. Develop. Drugs 06 (01). https://doi.org/10.4172/2329-663110.4172/2329-6631.1000167.

Lauer, M.K., Smith, R.C., 2020. Recent advances in starch-based films toward food packaging applications: Physicochemical, mechanical, and functional properties. Compr. Rev. Food Sci. Food Saf. 19 (6), 3031–3083. https://doi.org/10.1111/1541-4337.12627.

Llanes, L., Dubessay, P., Pierre, G., Delattre, C., Michaud, P., 2020. Biosourced polysaccharide-based superabsorbents. Polysaccharides 1 (1), 51–79. https://doi.org/10.3390/polysaccharides1010005.

Lu, B., Lv, X., Le, Y., 2019. Chitosan-modified PLGA nanoparticles for control-released drug delivery. Polymers. 11, 304–304, 10.3390/polym11020304.

Luo, Y., Chen, X., Luo, L., Zhang, Q.i., Gao, C., Zhuang, X., Yuan, S., Qiao, T., 2018. [6]-Gingerol enhances the radiosensitivity of gastric cancer via G2/M phase arrest and apoptosis induction. Oncol. Rep.. https://doi.org/10.3892/or.2018.629210.3892/or.2018.6292.

Mahady, G.B., Pendland, S.L., Yun, G.S., et al., 2003. Ginger (Zingiber officinale Roscoe) and the gingerols inhibit the growth of Cag A+ strains of Helicobacter pylori. Anticancer Res. 23, 3699–3702.

Matteucci, M.E., Miller, M.A., Williams, R.O., Johnston, K.P., 2008. Highly supersaturated solutions of amorphous drugs approaching predictions from configurational thermodynamic properties. J. Phys. Chem. B 112 (51), 16675–16681. https://doi.org/10.1021/jp805991f.

Mehta, M., Neeta, Pandey, P., Mahajan, S., Satija, S., 2018. Gastro retentive drug delivery systems: An overview. Res. J. Pharm. Technol. 11 (5), 2157. https://doi.org/10.5958/0974-360X.2018.00398.0.

Mircioiu, C., Voicu, V., Anuta, V., Tudose, A., Celia, C., Paolino, D., Fresta, M., Sandulovici, R., Mircioiu, I., 2019. Mathematical modeling of release kinetics from supramolecular drug delivery systems. Pharmaceutics 11 (3), 140. https://doi.org/10.3390/pharmaceutics11030140.

Patil, S., Pandit, A., Godbole, A., Dandekar, P., Jain, R., 2021. Chitosan based co-processed excipient for improved tableting. Carbohydrate Polymer Technologies and Applications. 2, 100071. https://doi.org/10.1016/j.carpta.2021.100071.

Pérez-Álvarez, L., Ruiz-Rubio, L., Lizundia, E., et al., 2018. Polysaccharide-based superabsorbents: Synthesis, properties, and applications. Springer International Publishing, Cellulose-based superabsorbent hydrogels.

Prajapati, V.D., Jani, G.K., Khutliwala, T.A., Zala, B.S., 2013. Raft forming system—An upcoming approach of gastroretentive drug delivery system. J. Control. Release 168 (2), 151–165. https://doi.org/10.1016/j.jconrel.2013.02.028.

Rajeswari, A., Gopi, S., Jackcina Stobel Christy, E., Jayaraj, K., Pius, A., 2020. Current research on the blends of chitosan as new biomaterials. In: Handbook of Chitin and Chitosan. Elsevier, pp. 247–283. https://doi.org/10.1016/B978-0-12-817970-3.00009-2.

Reyad-ul-ferdous, M., Shamim Shahjahan, D.M., M. Munirul Islam Tanvir,, et al., 2015. Effective development and evaluation of oral thin film of etoricoxib. World J. Pharm. Res. 4, 257–272.

Saal, W., Ross, A., Wyttenbach, N., Alsenz, J., Kuentz, M., 2017. A systematic study of molecular interactions of anionic drugs with a dimethylaminoethyl methacrylate copolymer regarding solubility enhancement. Mol. Pharm. 14 (4), 1243–1250. https://doi.org/10.1021/acs.molpharmaceut.6b0111610.1021/acs.molpharmaceut.6b01116.s001.

Sah, B.K., Lakshmi, C.S.R., Bukka, R., et al., 2020. Formulation and evaluation of folding film in a capsule for gastroretentive drug delivery system of losartan potassium. International Journal of Pharma and Chemical Research. 6, 1–8. https://doi.org/10.13140/RG.2.2.36375.19363.

Santos, V.P., Marques, N.S.S., Maia, P.C.S.V., Lima, M.A.B.d., Franco, L.d.O., Campos-Takaki, G.M.d., 2020. Seafood waste as attractive source of chitin and chitosan production and their applications. Int. J. Mol. Sci. 21 (12), 4290. https://doi.org/10.3390/ijms21124290.

Sato, H., Ogino, M., Yakushiji, K., Suzuki, H., Shiokawa, K.-I., Kikuchi, H., Seto, Y., Onoue, S., 2017. Ginger extract-loaded solid dispersion system with enhanced oral absorption and antihypothermic action. J. Agric. Food. Chem. 65 (7), 1365–1370. https://doi.org/10.1021/acs.jafc.6b0474010.1021/acs.jafc.6b04740.s001.

Sevinç özakar, R., Özakar, E., 2021. Current overview of oral thin films. Turkish Journal of Pharmaceutical Sciences. 18 (1), 111–121. https://doi.org/10.4274/tjps.galenos.2020.76390.

Singletary, K., 2010. Ginger. Nutr. Today 45, 171–183. https://doi.org/10.1097/NT.0b013e3181ed3543.

Sivaneswari, S., Karthikeyan, E., Chandana, P.J., 2017. Novel expandable gastro retentive system by unfolding mechanism of levetiracetam using simple lattice design – Formulation optimization and in vitro evaluation. Bulletin of Faculty of Pharmacy, Cairo University. 55 (1), 63–72. https://doi.org/10.1016/j.bfopcu.2017.02.003.

Soe, M.T., Pongjanyakul, T., Limpongsa, E., Jaipakdee, N., 2020. Modified glutinous rice starch-chitosan composite films for buccal delivery of hydrophilic drug. Carbohydr. Polym. 245, 116556. https://doi.org/10.1016/j.carbpol.2020.116556.

Srinivasan, K., 2017. Ginger rhizomes (Zingiber officinale): A spice with multiple health beneficial potentials. PharmaNutrition. 5 (1), 18–28. https://doi.org/10.1016/j.phanu.2017.01.001.

Tester, R. F. and W. R. Morrison, 1990. Swelling and gelatinization of cereal starches. I. Effects of amylopectin, amylose, and lipids'..

Thomas, F., 2020. Improving solubility with amorphous solid dispersions. Pharm. Technol. 44, 32–33.

Vrettos, N.-N., Roberts, C.J., Zhu, Z., 2021. Gastroretentive technologies in tandem with controlled-release strategies: A potent answer to oral drug bioavailability and patient compliance implications. Pharmaceutics. 13 (10), 1591. https://doi.org/10.3390/pharmaceutics13101591.

Wagner, J.G., 1989. Relationships between First-Order and Michaelis—Mentnen Kinetics. J. Pharm. Sci. 78 (6), 521–522. https://doi.org/10.1002/jps.2600780622.

Wang, B., Wang, D., Zhao, S., Huang, X., Zhang, J., Lv, Y., Liu, X., Lv, G., Ma, X., 2017. Evaluate the ability of PVP to inhibit crystallization of amorphous solid dispersions by density functional theory and experimental verify. Eur. J. Pharm. Sci. 96, 45–52. https://doi.org/10.1016/j.ejps.2016.08.046.

Wannasarit, S., P. Puttarak, K. Kaewkroek, et al., 2019. Strategies for improving healing of the gastric epithelium using oral solid dispersions loaded with pentacyclic triterpene–rich Centella extract. AAPS PharmSciTech. 20, 277-277. https://doi.org/10.1208/s12249-019-1488-7.

Wittaya, T., 2012. Rice starch-based biodegradable films: Properties enhancement. In: Amer Eissa, A. (Ed.), Structure and Function of Food Engineering. InTech. https://doi.org/10.5772/47751.

Wu, Q., Zhang, L., 2001. Structure and properties of casting films blended with starch and waterborne polyurethane. Journal of Applied Polymer Science. 79, 2006–2013. https://doi.org/10.1002/1097-4628(20010314)79:11<2006::AID-APP1009>3.0.CO;2-F.

Wu, W.-C., P.-Y. Hsiao and Y.-C. Huang, 2019. Effects of amylose content on starch-chitosan composite film and its application as a wound dressing. Journal of Polymer Research. 26, 137-137. https://doi.org/10.1007/s10965-019-1770-0.

Xu, Y.X., Kim, K.M., Hanna, M.A., Nag, D., 2005. Chitosan–starch composite film: preparation and characterization. Ind. Crops Prod. 21 (2), 185–192. https://doi.org/10.1016/j.indcrop.2004.03.002.

Yuan, Y.i., Zhang, L., Dai, Y., Yu, J., 2007. Physicochemical properties of starch obtained from Dioscorea nipponica Makino comparison with other tuber starches. J. Food Eng. 82 (4), 436–442. https://doi.org/10.1016/j.jfoodeng.2007.02.055.